PHYSICAL REVIEW B **89**, 180404(R) (2014)

Electrical detection of direct and alternating spin current injected from a ferromagnetic insulator into a ferromagnetic metal

P. Hyde, Lihui Bai, D. M. J. Kumar, B. W. Southern, and C.-M. Hu*
Department of Physics and Astronomy, University of Manitoba Winnipeg, Canada R3T 2N2

S. Y. Huang, B. F. Miao, and C. L. Chien
Department of Physics and Astronomy, Johns Hopkins University, Baltimore, Maryland 21218, USA
(Received 12 September 2013; published 9 May 2014)

We report dual spin pumping in magnetic bilayers made of a ferromagnetic insulator yttrium iron garnet (YIG) and a ferromagnetic metal permalloy (Py). At the YIG ferromagnetic resonance (FMR), we detect a charge voltage in Py caused by YIG spin pumping. At the Py FMR, we measure the charge voltage generated by Py spin rectification. A striking simultaneous enhancement of both voltages is found at the equal resonance condition of both FMRs, which we attribute to dynamic coupling of the dual spin pumping. Our results demonstrate that Py enables electrical detection of both dc and ac spin currents in the spin pumping from YIG, which reveals an alternative path for developing insulator spintronics.

DOI: 10.1103/PhysRevB.89.180404 PACS number(s): 76.50.+g, 73.50.Pz, 84.40.−x, 85.75.−d

Developing new methods for generating and detecting spin currents has been the central task of spintronics. In the pioneering work of Johnson and Silsbee [1], the generation and detection of spin-polarized currents were both achieved through the use of ferromagnetic metals (FM). Recent breakthroughs reveal ferromagnetic insulators (FI) to be promising spin current sources, in which spin currents can be generated without the presence of any charge current [2,3]. In the groundbreaking experiment performed three years ago by Kajiwara *et al.* [2], electrical detection of the spin current generated by yttrium iron garnet [$Y_3Fe_5O_{12}$ (YIG)] was achieved by utilizing the heavy normal metal (NM) platinum (Pt), in which spin current was detected via the inverse spin Hall effect (ISHE). So far, consensus has not yet been achieved on a few outstanding issues related to the quantitative description of spin currents in Pt [4–7]. More spin detectors are highly desirable in insulator spintronics. Given the fact that FM are broadly used as spin detectors in both semiconductor [8,9] and metallic spintronics devices [1,10], it is of particular interest to develop new methods for detecting spin currents generated from an insulator using FM electrodes, which will make insulator-spintronics devices compatible with both semiconductor and metallic spintronics devices.

In this paper, we report the first dual spin pumping experiment on magnetic bilayers made of FM/FI structures, in which we use the ferromagnetic metal permalloy (Py) instead of Pt to detect both the dc and ac spin currents. Distinct from previous studies of spin pumping in FM/NM structures [11,12] where Py is usually considered as a spin injector, we demonstrate the dual functionality of Py as both a spin injector and detector, which enables the electrical detection of coupled spin pumping in FM/FI bilayers, as revealed by the striking effect of simultaneously enhanced dc voltages generated by the ferromagnetic resonance (FMR) of both Py and YIG at the equal-resonance condition. We attribute this effect to dynamic coupling of the dual spin pumping in FM/FI bilayers via ac spin currents. Our experiment verifies the recent theory of ac spin pumping [13], establishes an alternate method for electrical detection of ac spin currents, and advances the study of spin pumping from FM/NM [11,12] and FI/NM [14,15] structures to a type of spintronics device made of FM/FI bilayers.

We begin by explaining the basic concept, technique, and method. As shown in Fig. 1, let us consider a Py/YIG bilayer set in an external magnetic field **H** under microwave excitation. At the FMR field H_{YIG} of YIG, the precessing magnetization of YIG pumps nonequilibrium spins diffusing across the Py/YIG interface, which injects a dc and an ac spin current [13,16,17] into the Py. Similarly, at the FMR field H_{Py} of Py, both dc and ac spin currents are injected into the YIG.

The FMRs of both YIG and Py are electrically detected by measuring the charge voltages generated in Py. At the Py FMR, the voltage V_{SR} as shown in Fig. 1(a) is generated by the spin rectification effect [18,19] in Py, which produces a rectified dc voltage from the mixing of the microwave current and the oscillating anisotropic magnetoresistance of Py. Note that V_{SR} is proportional to the precession angle of the Py FMR [20]. At the YIG FMR, we expect that the voltage V_{SP} will be generated as shown in Fig. 1(b) by spin pumping since the spin current $\mathbf{j_s}$ can be converted into a dc voltage via the ISHE of Py which was discovered recently [21].

The focus of our study is on the FMRs at the equal-resonance condition set by $H_{YIG} = H_{Py}$. As shown in Fig. 1(c), such a condition is achieved by adjusting the **H** field direction, making use of the different magnetic anisotropies of Py and YIG. Choosing the x axis as the longitudinal direction for measuring the dc voltages, and the z axis as perpendicular to the interface, the direction of **H** is described by the polar (with respect to the z axis) and azimuth (with respect to the x axis) angles of θ and ϕ, respectively. Since in general both spin rectification (V_{SR}) and spin pumping (V_{SP}) voltages contribute to the measured charge voltage, in order to clearly analyze them, we use a symmetry method developed very recently [20]

*hu@physics.umanitoba.ca

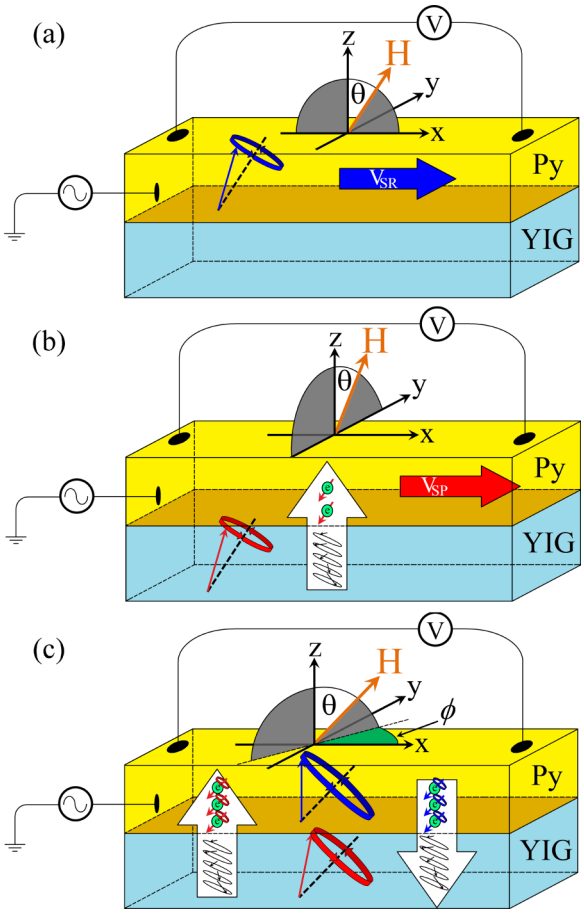

FIG. 1. (Color online) The FMR of (a) Py and (b) YIG can be detected by measuring V_{SR} via the spin rectification effect, and V_{SP} via the spin pumping effect, respectively. (c) At the equal-resonance condition, the ac spin current pumped from the YIG enhances the FMR of Py, which can be detected by the increased V_{SR}. Correspondingly, enhanced YIG FMR can be detected via the increased V_{SP}.

to identify V_{SP} and V_{SR}:

$$\begin{aligned} &At\ \phi = 0^\circ,\ V_{SP} = 0,\ V_{SR}(H) = V_{SR}(-H) \neq 0; \\ &At\ \phi = 90^\circ,\ V_{SR} = 0,\ V_{SP}(H) = -V_{SP}(-H) \neq 0. \end{aligned} \tag{1}$$

Samples were prepared by magnetron sputtering and patterned using a photolithography and liftoff technique. A Py thin film with the thickness d was deposited on a YIG substrate (10 mm × 4 mm × 0.5 mm) and patterned into a Hall bar structure with lateral dimensions of 5 mm × 0.2 mm. A 100-mW microwave was applied to excite FMR in the bilayer either through a rectangular waveguide or by sending a microwave current directly to the Py via a coaxial cable. By sweeping the **H** field at a fixed microwave frequency ω, dc voltages induced by FMR were detected along the longitudinal (x) axis of the Hall bar using lock-in amplification. Here, the microwave power was modulated at a frequency of 8.33 kHz.

Figure 2 shows typical voltage signals measured at $\omega/2\pi = 11$ GHz on a sample with $d = 10$ nm. While sweeping the **H** field applied at $\phi = 90^\circ$, we observe a background signal of ± 0.25 μV and sharp resonances at $\mu_0 H_R = \pm 0.484$ T with

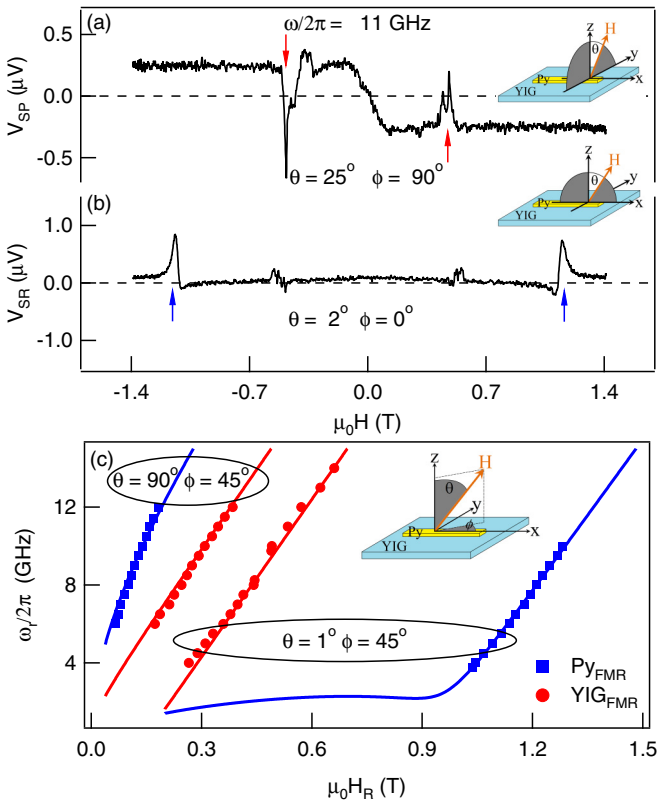

FIG. 2. (Color online) (a) The YIG and (b) the Py FMR electrically detected via V_{SP} at $\phi = 90^\circ$ and V_{SR} at $\phi = 0^\circ$, respectively. (c) The field dispersions of the Py and YIG FMRs measured at in-plane ($\theta = 90^\circ$) and out-of-plane ($\theta \approx 0^\circ$) field configurations. Curves are calculated theoretically.

a linewidth of 6.0 mT as shown in Fig. 2(a). At the lower (inner) field side of the sharp resonance, there is a weaker resonance together with a series of resonances too weak to be accurately distinguished. Both the background and resonance signals have an odd symmetry with respect to the **H** field direction, i.e., $V(H) = -V(-H)$. The data plotted in Fig. 2(a) were taken at $\theta = 25^\circ$, but data with an odd symmetry were measured at other angles of θ (not shown), provided $\phi = 90^\circ$. In contrast, by setting $\phi = 0^\circ$, both the background and the two sharp resonances nearly disappear, as shown in Fig. 2(b). Instead, broader resonances at ± 1.137 T with a linewidth of 17.5 mT are observed, which have an asymmetric line shape but even field symmetry of $V(H) = V(-H)$. Again, as long as $\phi = 0^\circ$, the broad resonances with even field symmetry are observed at arbitrary angles of θ, but note that they do not appear in the spectrum measured at $\phi = 90^\circ$.

The background signal V_{bg} is caused by thermal effects since, in general, for devices with a thin metallic layer deposited on a thick substrate, microwave heating is known to cause a temperature gradient perpendicular to the interface [22]. With such a vertical temperature gradient, two mechanisms may both cause V_{bg}: (i) the anomalous Nernst effect [5], (ii) the spin Seebeck [7] and ISHE effect [21]. Both mechanisms have the same angular dependence of $V_{bg} \propto \sin(\phi)$ as found in our measurements. Similar background voltage V_{bg} has been observed in other bilayer devices such as Pt/YIG under microwave excitation [23].

Both the sharp and broad resonances are caused by the charge voltages of the FMR. When $\phi \neq n\pi/2$ where n is an integer, we find that both resonances appear in the same voltage trace. Although their relative strength depends on ϕ, as we have discussed, neither of their resonance fields is sensitive to this angle; both depend on the polar angle θ. Setting $\phi = 45^\circ$, the dispersions for both resonances were measured at $\theta = 1^\circ$ and 90°, corresponding to perpendicular and in-plane **H** field directions, respectively. They are plotted in Fig. 2(c) for comparison. To identify these resonances, we have calculated the FMR conditions for the Py/YIG bilayer by linearizing the Landau-Lifshitz-Gilbert equations about the equilibrium determined by the **H** field strength and direction. Because of the macroscopic lateral size of the device, we model the magnetic anisotropy using a perpendicular demagnetization field $\mu_0 M_d$ as the fitting parameter. From the best fits we find $\mu_0 M_d = 0.147$ and 0.910 T for YIG and Py, respectively. The gyromagnetic factor is found to be $\gamma = 27.0$ and 26.2 GHz/T for YIG and Py, respectively. Note that the thin Py film has a much larger perpendicular anisotropy than YIG, as expected. The calculated dispersions are plotted in Fig. 2(c) as solid curves. The good agreement allows us to identify the sharp and broad resonances in Figs. 2(a) and 2(b) as the FMRs of YIG and Py, respectively. To keep the focus, our calculation includes neither exchange coupling nor the high-order anisotropies of YIG, hence it does not explicitly explain the origin of the weak resonance in Fig. 2(a), which could be a spin wave observed previously [2].

From Eq. (1), at $\phi = 90^\circ$, the measured field symmetry of $V(H_{\rm YIG}) \simeq -V(-H_{\rm YIG})$ as shown in Fig. 2(a) allows us to identify the dc voltage of the YIG FMR as $V_{\rm SP}$ [20]. This demonstrates that the dc spin current $\mathbf{j_s}$ injected from the YIG into the Py is electrically detected via spin pumping. Similarly, at $\phi = 0^\circ$, the measured field symmetry of $V(H_{\rm Py}) \simeq V(-H_{\rm Py})$ as shown in Fig. 2(b) confirms that the Py FMR is electrically detected via spin rectification [18,20].

We now use the electrically detected FMRs to study the coupling of dual spin pumping at the equal resonance condition of FM/FI bilayers. As shown in Fig. 2(c), at the same microwave frequency, the Py FMR measured in the in-plane configuration with $\theta = 90^\circ$ appears on the low-field side of the YIG FMR. Due to the larger perpendicular anisotropy of Py, in the perpendicular configuration with $\theta = 1^\circ$, the Py FMR moves to the high-field side. Hence, the equal-resonance condition of Py and YIG can be set by tuning the polar angle θ. With the obtained parameters, we have calculated and found that the equal-resonance condition occurs at $\theta = 12^\circ$.

According to Eq. (1), we trace at $\phi = 90^\circ$ the electrically detected FMR of YIG measured at $\omega/2\pi = 7$ GHz when θ is tuned through 12°. As shown in Fig. 3(a), the YIG FMR signal $V_{\rm SP}$ is seen to increase from 9° to 12° by about a factor of 2 (from 0.15 μV to above 0.3 μV). When θ is further tuned from 12° to 15.6°, the FMR signal amplitude drops back below 0.1 μV. Similarly, by setting $\phi = 0^\circ$, we trace the electrically detected FMR of Py. As shown in Fig. 3(b), when θ is tuned from 9° to 12°, the peak-to-peak amplitude of the Py FMR signal $V_{\rm SR}$ is seen to increase by more than a factor of 4 (from below 0.5 μV to above 2 μV). When θ is further tuned from 12.0° to 15.6°, the FMR signal amplitude drops back below 2 μV. Note that the symmetry method of Eq. (1) was

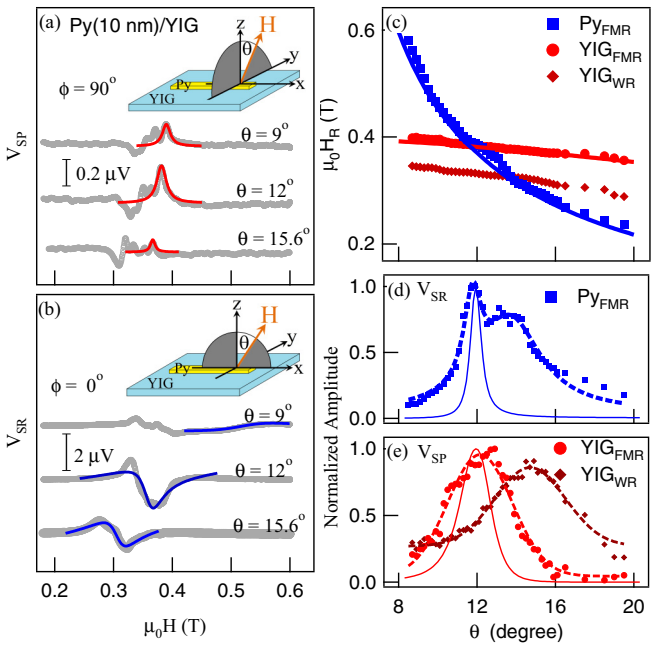

FIG. 3. (Color online) (a) YIG and (b) Py FMR measured at $\omega/2\pi = 7$ GHz near $\theta = 12^\circ$. (c) The polar angular dependence of the resonance fields showing the Py FMR crossing the YIG resonances at $\theta = 12^\circ$ and 14°. The normalized amplitudes of (d) the Py and (e) the YIG FMR voltages showing the simultaneous enhancement at equal-resonance conditions. Solid curves in (a) and (b) are from fitting, solid curves in (c), (d), and (e) are calculated theoretically, dashed curves in (d) and (e) are a guide to eyes.

developed for the FMR [20]. In Fig. 3(a), the $V_{\rm SP}$ data of the spin waves appearing at the low-field side of the YIG FMR are complicated. Since there is no theory for distinguishing spin pumping and rectification for YIG spin waves, we focus on analyzing the FMR signals highlighted by the thin curves. In Fig. 3(b), the detailed line shape of the Py FMR depends sensitively on the external field direction [24,25], but at $\phi = 0^\circ$ the amplitude of $V_{\rm SR}$ provides a good measure of the amplitude of the magnetization precession of Py [20].

The enhanced FMR voltages at $\theta = 12^\circ$ can be more clearly seen from the systematic data summarized in Figs. 3(c)–3(e). As shown in Fig. 3(c), going from the perpendicular down to the in-plane configuration by increasing θ, the FMR field of Py deceases much faster than that of YIG due to their different perpendicular anisotropies. It crosses first at $\theta = 12^\circ$ with the YIG FMR (as calculated), then it crosses at about 14° with the weak resonance mode $\rm YIG_{WR}$. Figure 3(d) shows the amplitude of the Py FMR signal measured at $\phi = 0^\circ$ via spin rectification, which is normalized by its maximum amplitude of 2.67 μV at $\theta = 12^\circ$. For comparison, the amplitude of the YIG FMR measured at $\phi = 90^\circ$ via spin pumping is plotted in Fig. 3(e), which is normalized by its maximum amplitude of 0.35 μV, also at $\theta = 12^\circ$. Clearly, the amplitudes of both the Py and YIG FMR voltages increase dramatically and simultaneously at the equal-resonance condition. Another key feature is that the angular range of the enhanced Py FMR is smaller than that of YIG, which is intriguing since the linewidth of Py FMR is broader than YIG FMR.

The simultaneous enhancement of both FMR voltages is distinct from the anticrossing of optical and acoustic FMR modes caused by magnetic coupling [26], which would lead to the enhancement of one mode accompanied by the suppression of the other. Here, we develop a simple model to highlight the underlying physics of coupled dual ac spin pumping in FM/FI bilayers.

Based on the recent theory of ac spin pumping [13], the YIG FMR driven by the microwave magnetic field $h(\omega t)$ injects an ac spin current $j_a(\omega t)$ into Py. The amplitude of the ac spin current $j_a \propto \chi_{\rm YIG}$ [13], where $\chi_{\rm YIG}$ is the H-field dependent amplitude of the matrix element of the Polder tensor [19]. In the Py layer, the injected ac spin current provides a dynamic spin torque [27] on the Py magnetization, due to the dynamic exchange interaction between the Py magnetization and the ac spin current. In a crude approximation focusing on the resonant feature of the H-field dependence but neglecting the detailed phase information, the dynamic exchange interaction can be modeled [16] as an effective ac magnetic field $h_a(\omega t)$ acting on the Py magnetization, with the amplitude $h_a \propto j_a \propto \chi_{\rm YIG}(H)$. At the FMR of YIG, $h_a \gg h$ because of the large $\chi_{\rm YIG}$ and the strong exchange interaction between $j_a(\omega t)$ and the Py magnetization [16]. Hence, at the equal resonance condition, $h_a(\omega t)$ enhances the Py FMR detected through spin rectification. Simultaneously, the ac spin current pumped by Py enhances the YIG FMR, which is electrically detected through spin pumping. Using the general expressions for $V_{\rm SR}$ and $V_{\rm SP}$ [20], our simple model predicts $V_{\rm SR} \propto |\chi_{\rm Py}(H)\chi_{\rm YIG}(H)|$ at the Py FMR field ($H = H_{\rm Py}$), and $V_{\rm SP} \propto |\chi_{\rm YIG}(H)\chi_{\rm Py}(H)|^2$ at the YIG FMR field ($H = H_{\rm YIG}$). Using the FMR fields and linewidths experimentally measured at $\omega/2\pi = 7$ GHz, we determine $\chi(H)$ [19], from which the calculated $V_{\rm SR}$ and $V_{\rm SP}$ are plotted as solid curves in Figs. 3(d) and 3(e), respectively. Without any adjustable parameters, and despite the crude approximations, this simple model captures two intriguing key features of the observed coupling: (i) the simultaneous enhancement of $V_{\rm SR}$ and $V_{\rm SP}$ at the equal-resonance condition, and (ii) the fact that the angular range of the enhanced $V_{\rm SR}$ measured at Py FMR is narrower than that of $V_{\rm SP}$ measured at YIG FMR, despite the fact that the FMR of Py is broader than that of YIG.

The most distinctive feature of this simple model is that the dynamic coupling of dual spin pumping does not influence the effective fields that determine $H_{\rm Py}$ and $H_{\rm YIG}$. Hence, it predicts mode crossing instead of anticrossing. To investigate such a distinction more carefully, we measure systematically a series of samples with different Py thickness d. Enhancement of $V_{\rm SR}$ and $V_{\rm SP}$ are observed in all Py/YIG bilayers. In samples with a thin Py layer ($d = 10$, 14, and 20 nm), the enhanced FMR voltages of Py and YIG are separately measured at $\phi = 0^\circ$ and 90°, respectively, because at other angles of ϕ the overlapping of the YIG and Py signals make it difficult to unambiguously identify the broad FMR of Py, as indicated in Fig. 4(a) for the sample of d =10 nm measured at $\phi = 45^\circ$. However, we find that the linewidth of the Py FMR decreases with increasing d, so that in the sample of $d = 30$ nm, the overlapped FMRs of Py and YIG measured at $\phi = 45^\circ$ can be analyzed by line-shape fitting [24,25] as plotted in Fig. 4(b), which directly shows that the enhanced FMRs of Py and YIG cross each other at the equal-resonance condition (of about $\theta = 10^\circ$ for this sample). It directly confirms that the resonant coupling observed in our FM/FI bilayers is indeed distinctly different from the magnetic coupling induced anticrossing. We conclude that although our simple model may be further improved by taking into account more details such as interface dynamic pinning, the phase of spin torques, and the reduced damping at the equal-resonance condition [17], the qualitative agreement of the model with the key features of our experiment makes the underlying physics of dynamic coupling of dual spin pumping in FM/FI bilayers very plausible. We note that the ac spin current enhanced FMR resembles the enhanced transmission-electron-spin resonance discovered by Silsbee *et al.* [16].

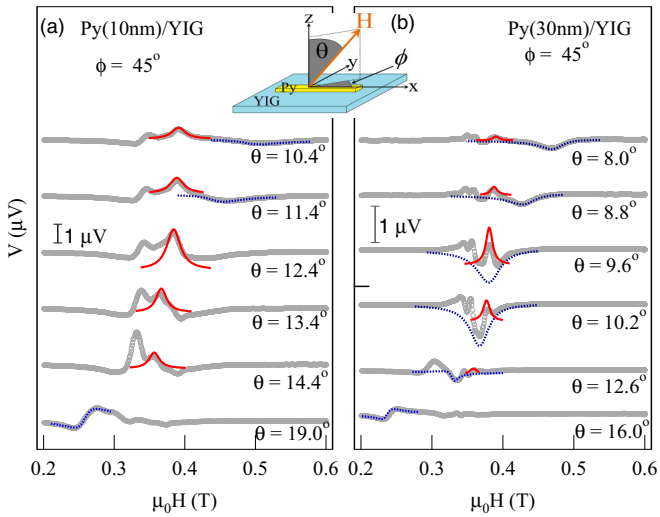

FIG. 4. (Color online) The polar angular dependence of the YIG and Py FMRs measured at $\omega/2\pi = 7$ GHz and $\phi = 45^\circ$ on samples with Py thickness of (a) 10 and (b) 30 nm. Solid and dashed curves are from the fitting of the YIG and Py FMR, respectively.

In summary, we have demonstrated alternate methods for the electrical detection of dc and ac spin currents in YIG. Both are achieved by using Py as the spin detector. Since the magnetization in Py is very easy to control by either tuning an external magnetic field or by tailoring its shape anisotropy, we expect that our methods will permit the advancement of insulator spintronics into a distinct path, which opens a significant area of studying the highly interesting topics of ac spin pumping [13], ac spin current [28–30], and ac spin torque.

Work in Manitoba has been funded by NSERC, CFI, URGP, and UMGF grants (C.-M.H. and B.W.S.). Work at JHU has been funded by NSF (Grant No. DMR-1262253). D.M.J.K was supported by Mitacs Globalink Program. S.Y.H was partially supported by STARnet sponsored by MARCO and DARPA.

[1] M. Johnson and R. H. Silsbee, Phys. Rev. Lett. **55**, 1790 (1985).

[2] Y. Kajiwara, K. Harii, S. Takahashi, J. Ohe, K. Uchida, M. Mizuguchi, H. Umezawa, H. Kawai, K. Ando, K. Takanashi,

S. Maekawa, and E. Saitoh, Nature (London) **464**, 262 (2010).

[3] Ken-ichi Uchida, Hiroto Adachi, Takeru Ota, Hiroyasu Nakayama, Sadamichi Maekawa, and Eiji Saitoh, Appl. Phys. Lett. **97**, 172505 (2010).

[4] S. Y. Huang, W. G. Wang, S. F. Lee, J. Kwo, and C. L. Chien, Phys. Rev. Lett. **107**, 216604 (2011).

[5] S. Y. Huang, X. Fan, D. Qu, Y. P. Chen, W. G. Wang, J. Wu, T. Y. Chen, J. Q. Xiao, and C. L. Chien, Phys. Rev. Lett. **109**, 107204 (2012).

[6] D. Qu, S. Y. Huang, Jun Hu, Ruqian Wu, and C. L. Chien, Phys. Rev. Lett. **110**, 067206 (2013).

[7] T. Kikkawa, K. Uchida, Y. Shiomi, Z. Qiu, D. Hou, D. Tian, H. Nakayama, X.-F. Jin, and E. Saitoh, Phys. Rev. Lett. **110**, 067207 (2013).

[8] C.-M. Hu, J. Nitta, A. Jensen, J. B. Hansen, and H. Takayanagi, Phys. Rev. B **63**, 125333 (2001).

[9] Xiaohua Lou *et al.*, Nat. Phys. **3**, 197 (2007).

[10] F. J. Jedema, H. B. Heersche, A. T. Filip, J. J. A. Baselmans, and B. J. van Wees, Nature (London) **416**, 713 (2002).

[11] Y. Tserkovnyak, A. Brataas, and G. E. W. Bauer, Phys. Rev. Lett. **88**, 117601 (2002).

[12] E. Šimánek and B. Heinrich, Phys. Rev. B **67**, 144418 (2003).

[13] H. J. Jiao and G. E. W. Bauer, Phys. Rev. Lett. **110**, 217602 (2013).

[14] B. Heinrich, C. Burrowes, E. Montoya, B. Kardasz, E. Girt, Young-Yeal Song, Yiyan Sun, and Mingzhong Wu, Phys. Rev. Lett. **107**, 066604 (2011); Appl. Phys. Lett. **100**, 092403 (2012).

[15] A. V. Chumak, V. I. Vasyuchka, A. A. Serga, M. P. Kostylev, V. S. Tiberkevich, and B. Hillebrands, Phys. Rev. Lett. **108**, 257207 (2012).

[16] R. H. Silsbee, A. Janossy, and P. Monod, Phys. Rev. B. **19**, 4382 (1979).

[17] B. Heinrich, Y. Tserkovnyak, G. Woltersdorf, A. Brataas, R. Urban, and G. E. W. Bauer, Phys. Rev. Lett. **90**, 187601 (2003).

[18] Y. S. Gui, N. Mecking, X. Zhou, Gwyn Williams, and C.-M. Hu, Phys. Rev. Lett. **98**, 107602 (2007).

[19] N. Mecking, Y. S. Gui, and C.-M. Hu, Phys. Rev. B **76**, 224430 (2007).

[20] Lihui Bai, P. Hyde, Y. S. Gui, C.-M. Hu, V. Vlaminck, J. E. Pearson, S. D. Bader, and A. Hoffmann, Phys. Rev. Lett. **111**, 217602 (2013).

[21] B. F. Miao, S. Y. Huang, D. Qu, and C. L. Chien, Phys. Rev. Lett. **111**, 066602 (2013).

[22] Z. H. Zhang, Y. S. Gui, L. Fu, X. L. Fan, J. W. Cao, D. S. Xue, P. P. Freitas, D. Houssameddine, S. Hemour, K. Wu, and C.-M. Hu, Phys. Rev. Lett. **109**, 037206 (2012).

[23] B. Hillebrands, S. Goennenwein, and J. Q. Xiao (private communication).

[24] A. Wirthmann, X. Fan, Y. S. Gui, K. Martens, G. Williams, J. Dietrich, G. E. Bridges, and C.-M. Hu, Phys. Rev. Lett. **105**, 017202 (2010).

[25] M. Harder, Z. X. Cao, Y. S. Gui, X. L. Fan, and C.-M. Hu, Phys. Rev. B **84**, 054423 (2011).

[26] B. Heinrich, Z. Celinski, J. F. Cochran, W. B. Muir, J. Rudd, Q. M. Zhong, A. S. Arrott, K. Myrtle, and J. Kirschner, Phys. Rev. Lett. **64**, 673 (1990).

[27] L. Liu, T. Moriyama, D. C. Ralph, and R. A. Buhrman, Phys. Rev. Lett. **106**, 036601 (2011).

[28] Dahai Wei, Martin Obstbaum, Mirko Ribow, Christian H. Back, and Georg Woltersdorf, Nat. Commun. **5**, 3768 (2014).

[29] C. Hahn, G. de Loubens, M. Viret, O. Klein, V. V. Naletov, and J. Ben Youssef, Phys. Rev. Lett. **111**, 217204 (2013).

[30] M. Weiler, J. M. Shaw, H. T. Nembach, and T. J. Silva, arXiv:1401.6469.